An integrated convolutional neural network-based surrogate model for crashworthiness performance prediction of hot-stamped vehicle panel components

Haoran Li[1], *Haosu* Zhou[1], and *Nan* Li[1*]

[1]Dyson School of Design Engineering, Imperial College London, Exhibition Road, London SW7 2AZ, UK

Abstract. During the structural design of vehicle components, Finite Element (FE) modelling has been extensively used for simulations of physical experiments. A typical design optimisation task requires iterative simulations to identify the optimum design, where FE simulations can be too time-consuming. Surrogate models have been developed to approximate complex simulations, which can reduce computational time and improve the efficiency of the design cycle. This paper presents a novel application of convolutional neural network (CNN) on rapid predictions of crashworthiness performance of vehicle panel components considering manufacturability. The dataset for training the model was generated based on the FE results of hot-stamped ultra-high strength steel (UHSS) B-pillar components. The formed components were analysed with a simplified lateral crash test to evaluate the deformation under impact. The trained model can instantly predict the deformation of the designed component with high accuracy compared to the FE results. Due to its high computational efficiency and precision, the surrogate model enables faster and more extensive design evaluations.

1 Introduction

Vehicle light-weighting has been a highly focused industrial priority for improving fuel efficiency and reducing emissions. During the structural design of vehicle components, various criteria such as manufacturing feasibility and crashworthiness performance must be considered in parallel to weight reduction. Hot-stamped ultra-high strength steels (UHSS) are widely used in vehicle safety-critical components like the A-pillar, B-pillar, and roof crossmembers. To ensure the quality and performance of the components, manufacturing constraints such as post-stamped thinning and wrinkling must be carefully considered in the design phase. In addition to the considerations of manufacturing feasibility, crashworthiness analysis is one of the most important performance metrics for vehicle safety-critical components. The primary objective of crashworthiness analysis is to assess how efficiently

* Corresponding author: n.li09@imperial.ac.uk

© The Authors, published by EDP Sciences. This is an open access article distributed under the terms of the Creative Commons Attribution License 4.0 (https://creativecommons.org/licenses/by/4.0/).

the components can absorb and dissipate energy during vehicular collisions, thereby minimising injury to the occupants.

The process of design optimisation of vehicle components often demands iterative trial-and-error methodologies. Traditional Finite Element (FE) simulations can become time-consuming with complex designs and advanced manufacturing processes. Machine learning (ML) empowered surrogate modelling has emerged as a promising solution to this limitation.

ML-based surrogate models have been utilised in conjunction with FE simulations for more efficient crashworthiness analyses. Rogala et al. [1] utilised the multilayer perceptron (MLP) to predict crashworthiness indicators for conical components under axial impact test. This model operates on a scalar basis, the inputs of the MLP are dimensional parameters, where the outputs are crashworthiness indicators like the mean crash force. Sakaridis et al. [2] used a similar MLP-based surrogate model for predicting the buckling behaviours of tubular structures based on force-displacement response. Kohar et al. [3] employed the long-short term memory (LSTM) neural networks to predict the crash pulse response in terms of acceleration measurements during the entire crash period of a pick-up truck.

Although scalar-based surrogate models can achieve rapid prediction with high accuracy, they cannot handle complex data forms. Crash simulations often involve complex deformation of components and field data like stress and strain distributions. Therefore, field-based surrogate models are developed for field data predictions. Kohar et al. [4] improved their model by employing a convolutional neural network (CNN) in conjunction with their LSTM-based surrogate model. A 3D-CNN-autoencoder was trained to process the FE mesh into latent vectors based on a voxelisation approach, which are then input into the LSTM-based surrogate model to predict desired outputs. The model can not only predict the time-series responses but also the component's deformation during crash tests. This voxelisation strategy is limited because it is only accurate for quadrilateral elements with constant size. Therefore, this model struggles to present complex components with unstructured meshes.

Highlighting the limitations of the previous ML-based surrogate models, this paper presents a novel application of CNN-based surrogate models for prediction of crashworthiness performance of vehicle panel components considering manufacturability. This integrated framework consists of two surrogate models, a hot stamping surrogate model (stamp model) and a crash simulation surrogate model (crash model). The stamp model takes in 2D projections of the tool shape design as input images, outputs the stamping results in terms of displacement fields of the blank, as well as the post-stamp thinning field. Such output images are then fed into the crash model, for prediction of the post-crash displacement fields. The workflow is illustrated in Figure 1. The complete framework provides a comprehensive analysis of the designed component's manufacturability and crashworthiness performance.

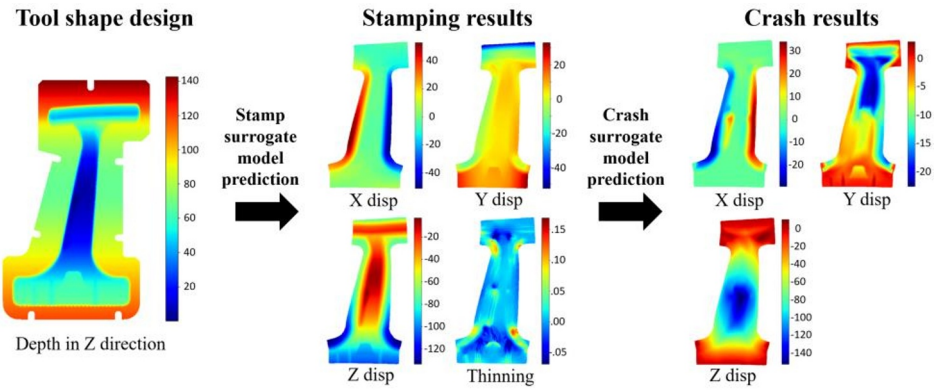


Fig. 1. Schematic workflow for the integrated surrogate models.

2 Data acquisition

2.1 Design of experiments and hot stamping FE simulations

The data for training the surrogate models was prepared with FE simulations. A hot-stamped UHSS B-pillar component is considered for this study. Data was created by varying the tool shape for stamping. 470 samples with different tool shapes were generated via mesh morphing with Hypermesh. Two regions, the T-joint and reinforcing rib areas were morphed with Latin hypercube sampling. The two areas were morphed within a range of 16mm and 8mm in the z direction, respectively. Figure 2 shows the mesh of a punch with the morphed areas highlighted with red lines. With these variations in tool shape, the formed component shape, thinning field, and post-crash deformation are all affected correspondingly. The 2D projection of the change in shape was generated as input to the stamp model.

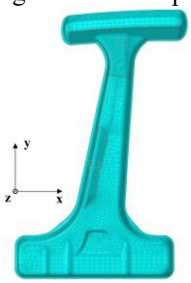


Fig. 2. Model of a punch with morphed area highlighted with red lines.

All morphed tools were imported to PAM-STAMP for stamping FE simulations. The tool shape was the only changing variable, the blank shape, material definition and all other processing parameters were fixed. The FE results were exported in terms of x, y, and z displacements and thinning fields. These fields were interpolated to the original blank shape to form the ground truth data for training the surrogate models. Details of the material definition, processing parameters and result interpolation can be found in [5].

2.2 Crash FE simulations

The predicted output from the hot stamping FE simulation was exported in terms of as-formed component mesh and thinning value for each element. After re-meshing the exported component with ideal uniform mesh configuration, it was assigned with strain-rate-dependent material properties of boron steel under the 100% martensite phase in room temperature. The material's constitutive model was developed by Li [6] as shown in Figure 3.

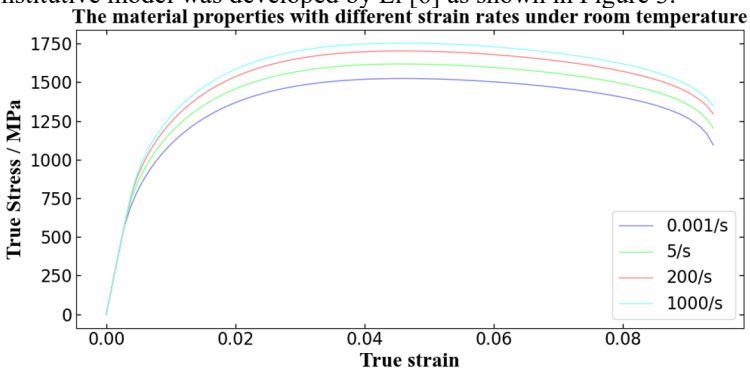


Fig. 3. Material properties of the studied UHHS at different strain rates.

The FE simulation aims to simplify the lateral impact test by the EuroNCAP standard. During the actual lateral impact test, a deformable barrier with a total mass of 1300 kg is driven into the testing vehicle at a velocity of 50 km/h. The centre of gravity of the impact barrier is 550 mm above the ground and the height of the frontal surface of the is approximately 600 mm. This impact was simplified as a distributed load of 140 kN exerting on an equivalent area on the B-pillar for a duration of 10 ms calculated from Equation (1):

$$F = \frac{(V \times m)}{t} \times 80\% \quad (1)$$

where F is the total force magnitude, V is the impact velocity, m is the mass of the impactor and t is the impact duration time. The calculated force was reduced by 20% due to the deformability of the impact barrier [7]. Figure 4 a) illustrates the boundary and loading conditions applied on the component, where the pink region indicates the distributed load, and the red region shows the fixed boundary conditions at the top and bottom edges of the component. The crash FE simulations were performed with PAM-CRASH. The thickness distribution was mapped to the re-meshed pre-crash mesh model from the post-stamp result in order to achieve realistic simulation with thickness variations.

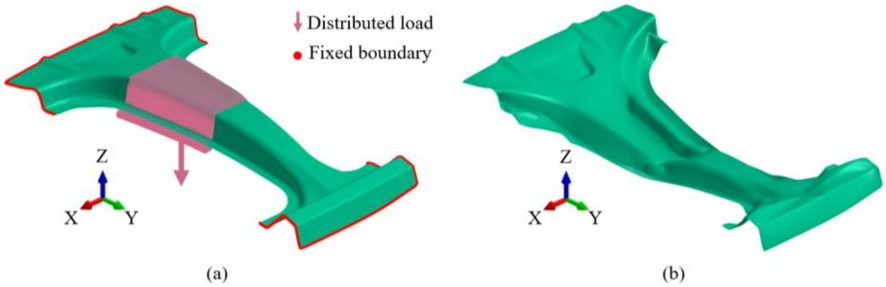


Fig. 4. Illustration of a) boundary and loading conditions on the B-pillar, b) the resultant deformation.

After completion of the FEM simulations, the x, y, and z displacement fields were extracted and mapped onto 2D images in the form of contour plots. In order to achieve the projection with minimum loss of information, the deformed components need to be unfolded into the original blank shape. After unfolding, the extracted crash results can be mapped onto 2D images by interpolation between the structured grid and the unfolded mesh. The images were then used to train the CNN-based crash surrogate model.

3 CNN-based surrogate model for crashworthiness analysis

The CNN-based surrogate model for crashworthiness analysis consists of a Res-SE-U-Net architecture, combining residual connections and attention mechanisms with a U-Net. A detailed illustration of the Res-SE-U-Net model is shown in Figure 5. The architecture can be divided into three parts: down-sampling encoder, processor, and up-sampling decoder. The encoder takes in input images and performs down-sampling by 6 integrated convolutional layers as illustrated in blue arrows in Figure 5. The integrated convolutional layers consist of 2D convolutional layers followed by batch normalisation (BN) layers and rectified linear unit (ReLU) activation. The processor consists of 6 Res-SE blocks, consisting of 2 integrated convolutional layers followed by a squeeze-excitation (SE) block [8] with residual connection. The decoder consists of 6 up-sampling integrated convolutional layers followed by a final output layer. More details on the architecture can be found in [9, 10].

The input images of this surrogate model are the post-stamp x, y, and z displacement fields with the thinning field of each sample. The input images with a size of 4×1090×610 (channel number × height × width) are gradually downscaled and convolved by a factor of 2 to a size of 128×18×20 before entering the Res-SE-blocks. The output images are post-crash

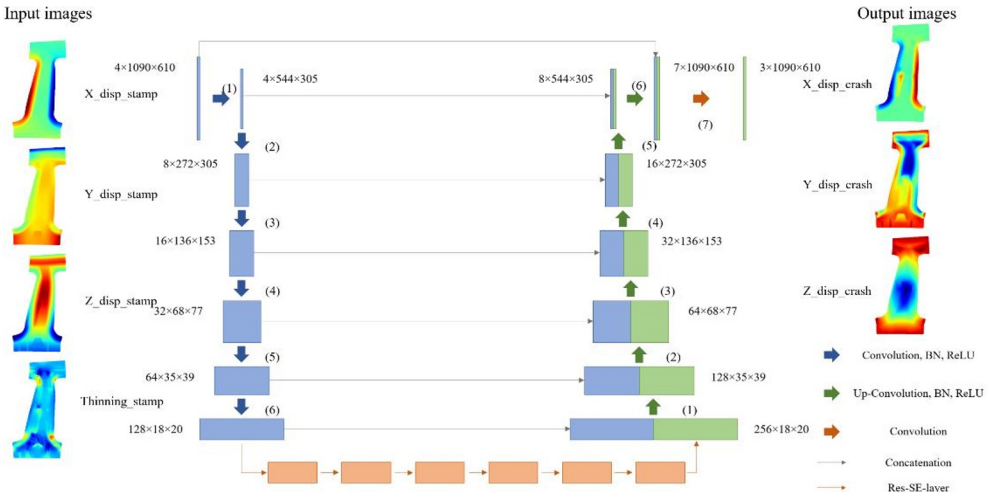


Fig. 5. Schematic of the Res-SE-U-Net architecture for crash model.

x, y, and z displacement fields, which were compared with the ground truth obtained from FEM to calculate loss functions. The loss function was defined as a combination of the Cosine similarity and the Euclidean distance loss function.

Similar architecture was used for the stamp model, more details can be found in [5, 11].

4 Training results and discussion

Both the stamp and crash models were separately trained with a train, validation, and test set of 400, 50, and 20 samples in total. After training, the stamp model was able to accurately predict the post-stamp displacement and thinning fields given the tool shape projection. The crash model was trained with FE ground truth as input images and output the predicted post-crash displacement fields. After training both models with ground truth data, the overall accuracy was evaluated by comparing the final crash predictions with the FE results when only inputting the tool shape projection images. Figure 6 shows a representative example comparison between the ground truth and the prediction. A good agreement between the prediction and ground truth contour plots can be visualised for all channels.

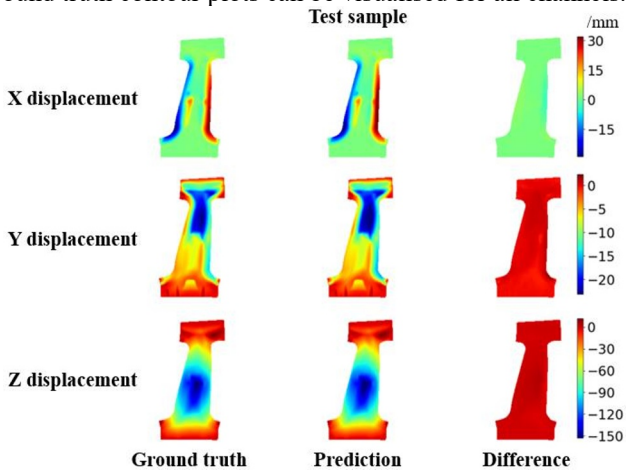


Fig. 6. Example comparison between the ground truth and surrogate model prediction.

For maximum x, y and z displacement predictions, the average relative errors are 2.04%, 3.05%, and 1.89%, respectively. As one of the most important measurements for crashworthiness, the z displacement represents the B-pillar intrusion after crash. This result shows that the model is capable of capturing the effect of change in tool shape design, which represents the change in component design, on the as-formed component's crashworthiness performance. One of the merits of this integrated surrogate model is that it predicts the manufacturability as an intermediate prediction which can lead to more comprehensive analyses.

5 Conclusion

An integrated CNN-based surrogate model was constructed and evaluated for manufacturability and crashworthiness performance prediction. This model connects the manufacturability and crashworthiness considerations for vehicle panel component dynamics prediction. The trained CNN-based surrogate model for crashworthiness analysis is able to accurately predict the impact behaviours of previously unseen hot-stamped B-pillar components under lateral impact test. In addition to the displacement fields, the model shows potential in predicting any field data, such as stress and strain fields, which can be used for more advanced crashworthiness analysis. This integrated framework can also be used in multi-objective optimisation tasks for structural design of any vehicle panel components.

Acknowledgements

The authors would like to thank ESI Group for technical support for PAM-STAMP and PAM-CRASH software. The authors also thank Innovate UK for the smart grant. For the purpose of open access, the authors have applied a Creative Commons Attribution (CC BY) license to any Author Accepted Manuscript version arising.

References

1. M. Rogala, J. Gajewski, M. Ferdynus, Materials **13**, 4857 (2020)
2. E. Sakaridis, N. Karathanasopoulos, D. Mohr, Int. J. Impact Eng., **166** (2022)
3. C. P. Kohar, D. S. Connolly, T. Liusko, K. Inal, MATEC Web Conf., **326**, 1006 (2020)
4. C. P. Kohar, L. Greve, T. K. Eller, D. S. Connolly, K. Inal, Comput. Method Appl. M., **385** (2021)
5. H. Zhou, N. Li, *Image-based Artificial Intelligence empowered surrogate model and shape morpher for real-time blank shape optimisation in the hot stamping process*, Arxiv preprint (2022)
6. N. Li, *Fundamentals of Materials Modelling for Hot Stamping of UHSS Panels with Graded Properties*, Ph.D. dissertation, Dept. of Mech. Eng., IC. (2013)
7. T. Baskara, M. Cimendag, Eylem, E. Yilmaz Ulu, JoCREST, **7**, 1-18 (2021)
8. J. Hu, L. Shen, G. Sun, CVPR, 7132-7141 (2018)
9. H. Zhou, Q. Xu, Z. Nie, N. Li, J. Manuf. Sci. Eng., **144**, 2 (2021)
10. H. R. Attar, H. Zhou, A. Foster, N. Li, J. Manuf. Process, **68**, 1650-1671 (2021)
11. H. R. Attar, H. Zhou, N. Li, IOP Conf. MSE, **1157**, 1 (2021)